International Journal of Nanomedicine

Dovepress
Taylor & Francis Group

Open Access Full Text Article

ORIGINAL RESEARCH

Enhancing Periodontal Ligament Regeneration via PDLSC Delivery Using Electrospun PCL/Collagen/Cellulose Acetate Scaffolds and Collagen Hydrogel Incorporated with Curcumin-Loaded ZIF-8 Nanoparticles

Xiaomin Lan[1,*], Yi Wang[2,*], Ming Yin[3,4]

[1]Department of Stomatology, The First Hospital of Shanxi Medical University, Taiyuan, Shanxi, 030001, China; [2]Department of Stomatology, The Second People's Hospital of Taiyuan, Taiyuan, 030002, China; [3]Department of Stomatology, Shanxi Bethune Hospital, Shanxi Academy of Medical Science, Tongji Shanxi Hospital, Third Hospital of Shanxi Medical University, Taiyuan, 030032, China; [4]Department of Stomatology, Tongji Hospital, Tongji Medical College, Huazhong University of Science and Technology, Wuhan, 430030, China

*These authors contributed equally to this work

Correspondence: Ming Yin, Email yinm0616@163.com

Background: Regenerating periodontal ligament (PDL) tissue is a vital challenge in dentistry that aims to restore periodontal function and aesthetics. This study explores a tissue engineering strategy that combines polycaprolactone (PCL)/collagen/cellulose acetate electrospun scaffolds with collagen hydrogels to deliver curcumin-loaded ZIF-8 nanoparticles fand periodontal ligament stem cells (PDLSCs).

Methods: Scaffolds were fabricated via electrospinningand collagen hydrogels incorporated PDLSCs and curcumin-loaded ZIF-8 nanoparticles (CURZIF-8) were developed using cross-linking. In vitro assays evaluated biocompatibility, anti-inflammatory, and antioxidative properties. In vivo efficacy was assessed in a rat PDL injury model using histological and ELISA analyses examining tissue regeneration and inflammatory cytokine modulation.

Results: In vitro studies demonstrated that the scaffolds effectively supported PDLSC viability and migration. CURZIF-8 hydrogels enhanced anti-inflammatory and antioxidative activities. In vivo study showed that the combined scaffold-hydrogel system significantly promoted PDL regeneration. Tissue levels of bFGF, HGF, and TGF-β that are crucial for tissue repair, angiogenesis, and cell proliferation were evaluated. Whereas, pro-inflammatory cytokines TNF-α and IL-6=were downregulated. Histological analysis confirmed the formation of organized PDL structures and improved bone-cementum integration that arekey indicators of successful periodontal regeneration.

Conclusion: The developed scaffold-hydrogel system facilitates PDL regeneration by modulating inflammation and promoting pro-healing factor expression. This approach shows promise for advancing periodontal tissue engineering and warrants further investigation in clinical settings.

Keywords: periodontal ligament regeneration, periodontal ligament stem cells, electrospun scaffolds, collagen hydrogel, curcumin, ZIF-8 nanoparticles, tissue engineering

Introduction

Periodontitis is primarily caused by bacterial biofilms such as *Porphyromonas gingivalis, Tannerella forsythia*, and *Treponema denticola* that colonize the gingival sulcus and trigger a host immune response.[1,2] This leads to chronic inflammation characterized by the release of pro-inflammatory cytokines like IL-1β, IL-6, and TNF-α that mediate the destruction of periodontal tissues. Thisincludes the periodontal ligament, alveolar bone, and cementum.[3–5] The

Received: 27 September 2024
Accepted: 15 December 2024
Published: 20 January 2025

Graphical Abstract

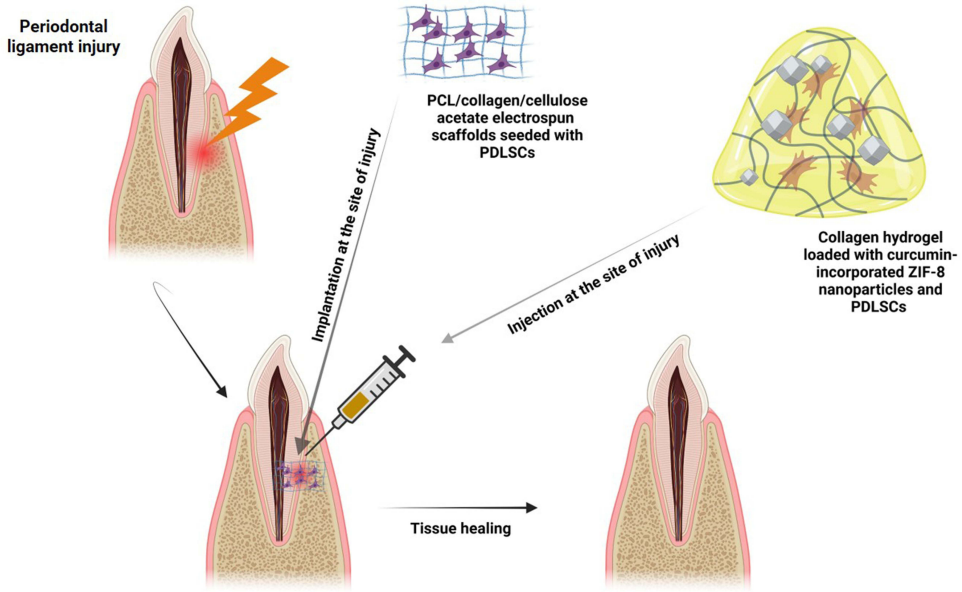

consequences of periodontitis extend beyond local tissue damage that result in periodontal bone loss and tooth loss that compromise both the esthetic and functional aspects of the oral cavity. This condition also affects mastication and speech that reduce the patient's quality of life. Traditional periodontal treatments such as scaling and root planning, guided tissue regeneration (GTR), and the use of barrier membranes, are effective in halting disease progression and promoting some tissue repair.[3,6] However, these approaches often fail to fully regenerate the intricate architecture of the periodontal apparatus that include the periodontal ligament, alveolar bone, and cementum as shown by incomplete restoration of lost tissue and compromised functional outcome studies that have shown that while GTR can lead to partial bone regeneration. Similarly, boned barrier membranes do not consistently achieve true periodontal regeneration involving new cementum and functional PDL fibers.[7,8] Given these challenges, periodontal regeneration aims not only to repair but also to fully restore the architecture and functionality of these tissues These objectives cannot be achieved by traditional therapies. Recent advancements in tissue engineering such as PDLSC delivery via biomaterial scaffolds offer a promising solution to these limitations.[9,10]

PDLSCs that are type of mesenchymal stem cells found within the periodontal ligament, have demonstrated the ability to differentiate into various cell types essential for periodontal regeneration such as osteoblasts, cementoblasts, and fibroblasts. Their potential for self-renewal and differentiation makes them ideal candidates for regenerative therapies aimed at restoring periodontal tissues.[11,12] However, the success of PDLSC-based therapies is heavily dependent on the development of suitable delivery systems that can support cell viability, proliferation, and differentiation.[13] One promising delivery system involves electrospun scaffolds composed of polycaprolactone (PCL), collagen, and cellulose acetate. Electrospinning is a versatile technique for creating nanofibrous scaffolds that closely resemble the ECM and provide a conducive environment for cell attachment and growth.[14–16] Polycaprolactone (PCL) which is a biodegradable polyester is widely used in tissue engineering due to its biocompatibility and mechanical properties. However, PCL alone often lacks the bioactivity required for optimal cellular responses.[17,18] By integrating PCL with natural polymers like collagen and cellulose acetate, a composite material is created that leverages the advantages of each component.[19] Collagen, the main structural protein in the ECM, promotes cell adhesion, proliferation, and differentiation.[20] Whereas, cellulose acetate offers additional mechanical strength and stability.[21] This composite scaffold not only mimics the

fibrous nature of the periodontal ligament but also provides a supportive niche for PDLSCs, enhancing their regenerative potential.

In addition to creating a supportive scaffold, addressing inflammation and microbial challenges is crucial for successful periodontal regeneration.[22] Curcumin possesses potent anti-inflammatory, antioxidant, and antimicrobial properties that make it a valuable agent in promoting periodontal regeneration.[23,24] However, curcumin's poor solubility and rapid degradation in physiological conditions limit its therapeutic efficacy.[25] To overcome these challenges, curcumin can be encapsulated in metal-organic frameworks (MOFs) such as Zeolitic Imidazolate Framework-8 (ZIF-8). ZIF-8 which are composed of zinc ions and imidazolate linkers and offers a high surface area and tunable porosity.[26,27] Encapsulating curcumin in ZIF-8 nanoparticles not only protects it from degradation but also ensures sustained and targeted release at the site of periodontal injury.[28]

To maximize the therapeutic potential, PDLSCs and curcumin-encapsulated ZIF-8 nanoparticles can be incorporated into a collagen hydrogel. Collagen hydrogels are known for their biocompatibility and ability to support cell migration and proliferation.[29,30] This combination enhances the therapeutic environment by providing sustained release of curcumin and a biomimetic scaffold for PDLSCs function to create a conducive environment for tissue regeneration.

The utilization of PDLSCs-seeded PCL/collagen/cellulose acetate scaffolds along with PDLSCs and curcumin-encapsulated ZIF-8 nanoparticles loaded in a collagen hydrogel represents a multifaceted approach to periodontal regeneration. The aim of the current research is to investigate the healing activity of this complex system in a rat model of periodontal ligament injury.

Methods and Materials

Fabrication of PCL/Collagen/Cellulose Acetate Electrospun Scaffolds

PCL (Mn80000, Sigma Aldrich, USA) was dissolved in HFIP (Merck, Germany) at 12 wt.% concentration for 12hours at room temperature. Then collagen (rat tail, Sigma Aldrich, USA) and cellulose acetate (Sigma Aldrich, USA) were added to the PCL solution at 10 w/w and 5 w/w%, respectively. Then, the polymeric solution was loaded into a disposable syringe (10 mL) and connected to an electrospinning pump. The electrospinning began by applying a positive charge (18 kV) to the polymer at feeding rate of 0.75 mL/hour. The needle gauge was 18 and the needle to collector distance was about 15 cm. The turning rate of the mandrel fluctuated between 500–600 rpm. After fabricating the samples, they were placed under vacuum for 6hours to remove residual solvents. Subsequently, the samples were thoroughly rinsed with PBS 5–7 times to ensure complete elimination of HFIP toxicity. The produced scaffolds were named PCLCOLCELL.

Fabrication of Curcumin-Loaded ZIF-8 Nanoparticles

ZIF-8 nanoparticles (Nanosadra, Tehran, Iran) were pre-heated at 600°C for 45minutes to dry the nanocarriers. These nanoparticles were then used to encapsulate curcumin (Sigma Aldrich, USA). The encapsulation process involved mixing a solution of curcumin (1 grams in 100 mL of ethanol) alongside 20 grams of ZIF-8 nanoparticles. The mixture was magnetically stirred for 48hours. The drug-loaded ZIF-8 nanoparticles were collected by centrifugation at 15,000× g for 60minutes and washed with deionized water. The resulting solutions were lyophilized for 48hours to obtain the drug-loaded ZIF-8 nanoparticles that were designated as CURZIF-8.

Preparation of Collagen Hydrogel Loaded with CURZIF-8 and PDLSCs

A collagen solution (rat tail, 2 mg/mL, Sigma Aldrich, USA) was mixed with three different concentrations of CURZIF-8: 1 w/w%, 2 w/w%, and 10 w/w% mixed for 1 hour on ice. Next, 500,000 PDLSCs (passage 3, ATCC) were added to the collagen/CURZIF-8 mixture at a 1:1 volume ratio and mixed for another hour. The resulting solution was then incubated at 37°C for 1 hour to allow auto-crosslinking. For the in vivo study, the collagen solution was removed from the ice and injected at the injury site. The prepared hydrogels loaded with 1 w/w%, 2 w/w%, and 10 w/w% CURZIF-8 nanoparticles were named as COLPDLSCZIF-8-1, COLPDLSCZIF-8-2, and COLPDLSCZIF-8-10, respectively.

Microstructure Studies

The microstructure of electrospun scaffolds and ZIF-8 nanoparticles was examined using SEM imaging. The samples were gold-coated for 250seconds and imaged under an accelerating voltage of 20 kV. For the collagen hydrogels, the hydrogel system was fixed in 3.7% formalin for 15minutes and then washed five times with phosphate-buffered saline (PBS). The tissues were then embedded in paraffin, sectioned into 5μm thick slices, and stained with Masson's trichrome (MT).

Cell Viability Assay

To assess cell viability, an MTT assay was performed. In summary, 100μL of the hydrogel system containing 7000 cells was placed into 96-well plates and maintained for a duration of 5 days. The cellular metabolic activity was evaluated on days 1, 3, and 5 using an MTT assay kit (Abcam, USA). Regarding the electrospun scaffolds, the constructs were cut to fit the dimensions of 96-well plates. The, they were sterilized with 70% ethanol for 1 hour, and subsequently rinsed thoroughly with sterile PBS. The samples were then allowed to dry under sterile conditions and incubated with FBS for 24hours. PDLSCs were then seeded onto the scaffolds at a density of 7000 cells per scaffold in 25μL of culture medium and cultured for 5 days. Cell viability was assessed on days 1, 3, and 5 using the MTT assay kit (Abcam, USA), according to the manufacturer's instructions. Control is the cells cultured on the tissue culture plate.

Anti-Inflammatory Assay

For this experiment, the hydrogels (200 μL containing 50000 PDLSCs) were placed in 24-well plates. Mouse macrophages (J774A.1 cell line, ATCC) were then seeded onto the hydrogels at a concentration of 30000 cells per cm^2 and cultured for three days. The cells were subsequently stimulated with 1μg/mL ultrapure LPS (Sigma Aldrich, USA) for 12 hours. Pro-inflammatory cytokines (TNF-α, IL-6, and IL-1) released by the cells were quantified using ELISA kits (Abcam, USA). All experiments were conducted in triplicate. Control is the cells cultured on the tissue culture plate.

Swelling Assay

The COLPDLSCZIF-8hydrogels with varying levels of CURZIF-8 were weighed and then submerged in 10 mL of DMEM (ThermoFisher, USA) with 10% FBS (Sigma Aldrich, USA) and 1% antibiotics (Sigma Aldrich, USA)and then incubated for 48hours. At various time intervals, the hydrogels were removed from the medium and weighed. The swelling capacity of the samples was determined using the following formula.

$$\text{Swelling}\,(\%)=\left(\frac{M0-M1}{M0}\right)\times 100$$

Where M0 is the weight of the samples before immersing in the culture media and M1 is their weight after the immersing.

Anti-Oxidative Assay

The radical scavenging activity of ZIF-8 and CURZIF-8 nanoparticles was assessed using the DPPH assay as described previously. For the free curcumin, it was dissolved in ethanol at various concentrations to create a stock solution. ZIF-8 and CURZIF-8 nanoparticles were suspended in distilled water at different concentrations. DPPH was prepared at a concentration of 0.1mM using methanol as the solvent. Serial dilutions of each sample were made and mixed with the DPPH solution in a 1:1 volume ratio. These mixtures were then incubated in the dark for 1 hour to allow for interaction between the samples and DPPH radicals. After incubation, the absorbance of each sample was measured at 517 nm. The radical scavenging activity of each sample was then determined using a previously described method.[31]

Cytoprotecting Assay Under Oxidative Stress

The cytoprotective function of COLPDLSCZIF-8hydrogels conditioned media on the L929 fibroblast cells (ATCC) was assessed using a method as described previously.[32] In short, 1 mL of hydrogels was submerged in 5 mL of full culture medium and maintained for three days. Afterward, the treated medium was collected and stored at −80 °C. For the

experiment, L929 cells (murine fibroblast cell line) were exposed to a 1:1 mixture of hydrogel-conditioned medium and fresh medium for 48hours. Subsequently, the culture medium was supplemented with 1% v/v H_2O_2 and the cells were incubated for one hour. Finally, cell viability was assessed using the MTT assay.

Release Assay

The release of curcumin from the CURZIF-8 nanoparticles was evaluated using UV-visible spectroscopy at a wavelength of 420 nm. In summary, 500 mg of the nanocarriers were suspended in 15 mL of PBS and left for seven days. At various intervals, 0.5 mL of the PBS was taken and its optical density was determined. Subsequently, 0.5 mL of fresh PBS was added back to the primary release medium. The cumulative drug release was then calculated using the following formula.

$$\text{Cumulative drug release}(\%) = \left(\frac{\textit{Amount of the released drug at each time point}}{\textit{Initial amount of the loaded drug}} \right) \times 100$$

Cell Migration Assay

The migratory behavior of PDLSCs (passage 3, ATCC) in response to the conditioned media from COLPDLSCZIF-8-1, COLPDLSCZIF-8-2, and COLPDLSCZIF-8-10hydrogels was assessed using an in vitro scratch assay. Briefly, the 1 mL of the hydrogels were immersed in 5 mL of complete media for three days. Then, their conditioned media was collected, filtered, and stored at −80 °C. PDLSCs were cultured in 24-well plates until confluent. A sterile pipette was used to create a straight scratch in the center of the wells and cell debris was removed by washing with PBS. The cells were then incubated with the conditioned media from the nanocomposite hydrogels for 48hours. Then, images of the scratch area were taken using a light microscope and analyzed with ImageJ software (NIH, USA) to determine the percentage reduction in wound size.

FTIR Assay

The characteristics of ZIF-8 and CURZIF-8 nanoparticles was examined through FTIR (Bruker). The FTIR analysis was conducted over a wavelength range of 400 to 4000 cm^−1. The reading encompassed both the fingerprint area and the regions specific to functional groups in the infrared spectrum.

In vivo Study

This study was approved by the Ethical Committee of Shanxi Bethune Hospital (Approval No. YXLL-2023-322). All procedures involving animals were reviewed and approved by the Institutional Animal Care and Use Committee by the of the Ethics Committee of Shanxi Province Hospital of Traditional Chinese medicine. Measures were taken to alleviate animal distress and limit the number of animals used. ARRIVE guidelines have been followed for the in vivo study. During the procedure, the animals were sedated with intraperitoneal injections of ketamine hydrochloride (80 mg/kg) and xylazine hydrochloride (10 mg/kg). The upper and lower jaws of the rats were operated individually to reveal the surgical area. A 2% lidocaine solution was administered at the surgical site to minimize pain. A vertical full-thickness incision was made on the proximal palatal side of the left maxillary first molars. Using round burs and ample saline irrigation, the cementum covering the roots, periodontal ligament (PDL), and alveolar bone were removed. Subsequently, a rectangular periodontal defect with dimensions of 3 mm × 2 mm × 1 mm was created. Then, the animals were randomly assigned into 5 groups (5 animals per group): 1- HYDELC-CELLs-CURZIF-8 groupin which a small piece of cell-laden electrospun scaffolds (300 × 300μm²) with about 15000 PDLSCs was inserted into the defect. Then, injecting 50μL (containing approximately 25000 PDLSCs) of COLPDLSCZIF-8-2hydrogels, 2- HYDELC-CURZIF-8 group in which the electrospun scaffolds and hydrogels with 2 w/w % CURZIF-8 nanoparticles but without PDLSCs were used to treat the defects, 3- HYDELC-CELLs group in which the animals were treated with cell-loaded electrospun scaffolds and hydrogels but without CURZIF-8, 4- negative control group in which the animals received no treatment post-injury, 5- sham control group in which surgery exposed the maxillary first molar along the alveolar ridge but no tooth defect was created. Table 1 summarizes study groups. After placing the scaffolds, the flap was repositioned and closed with absorbable sutures. The animals were monitored for 6weeks and then euthanized using an overdose of pentobarbital sodium and their jaws were carefully dissected to expose the experimental site. Using fine surgical

 https://doi.org/10.2147/IJN.S492274

Table 1 Summary of Study Groups in the in vivo Study

Group	Treatment
HYDELC-CELLs-CURZIF-8	Cell-laden electrospun scaffolds with CURZIF-8 nanoparticles and PDLSCs
HYDELC-CURZIF-8	Electrospun scaffolds with CURZIF-8 nanoparticles, without PDLSCs
HYDELC-CELLs	Cell-laden electrospun scaffolds without CURZIF-8
Negative Control	No treatment post-injury
Sham Control	Surgical exposure without creating a defect

instruments, the periodontal ligament (PDL) was meticulously removed from the root surfaces of the maxillary first molar by gently scraping the area to ensure complete collection of the tissue. All tissue samples were immediately fixed in 3.7% formalin (Merck, Germany) for 48 hours to preserve cellular and extracellular structures. Following fixation, the samples were embedded in paraffin. The paraffin-embedded tissues were sectioned at a thickness of 5μm using a microtome and then stained with Hematoxylin and Eosin (H&E) for general histological examination and Masson's trichrome for the evaluation of collagen and fibrous tissue. A histomorphometric analysis was conducted by an independent pathologist who was blind to the study, following a previously described method.[33]

ELISA Assay

After the animals were sacrificed, the periodontal ligament tissues were collected and processed to evaluate the expression of TGF-β, b-FGF, HGF, IL-6, and TNF-α. This was done using ELISA assay kits from Abcam (USA) according to the manufacturer's instructions.

Statistical Analysis

We employed parametric tests such as Student's -test and one-way ANOVA for r data that met the assumptions of normality and homogeneity of variances. One-way ANOVA was used to evaluate the effects of different scaffold compositions on cell viability, anti-inflammatory activity, and other key outcomes across multiple groups, with post hoc Tukey's tests that identified significant differences between individual groups. For direct comparisons between two experimental conditions, Student's -test was applied. Statistical significance was set at $p < 0.05$. Adjustments for multiple comparisons were made using Tukey's test to minimize Type I error. All analyses were performed using GraphPad Prism Version 5.

Results

Microstructure Studies

Results (Figure 1A–D) demonstrated that the PCLCOLCELL scaffolds were composed of smooth fibers with a web-like structure. The fibers remained intact without any disintegration or bead formation. Measurements indicated that the electrospun scaffolds had an average fiber diameter of approximately 1848.25 ± 453.19 nm.

SEM images of ZIF and CURZIF-8 nanoparticles (Figure 1E and F) showed that the particles had smooth plane surfaces with sharp edges. The average particle size for ZIF and CURZIF-8 nanoparticles was measured to be 84.19 ± 21.97 nm and 105.85 ± 43.83 nm, respectively (Figure 2).

Masson's Trichrome staining images (Figure 3) of the hydrogels showed that PDLSCs were evenly distributed throughout the hydrogel system and the scaffolds were composed of fibrous microstructure.

Cell Viability Assay Results

MTT assay results (Figure 4) indicated that COLPDLSCZIF-8-10hydrogels imparted significant toxicity towards PDLSCs on all of the studied time points. On day 1, the COLPDLSCZIF-8-1 and COLPDLSCZIF-8-2hydrogels had significantly higher cell viability than the PCLCOLCELL scaffolds. However, on days 3 and 5, differences between the PCLCOLCELL, COLPDLSCZIF-8-1 and COLPDLSCZIF-8-2 scaffolds were not significant.

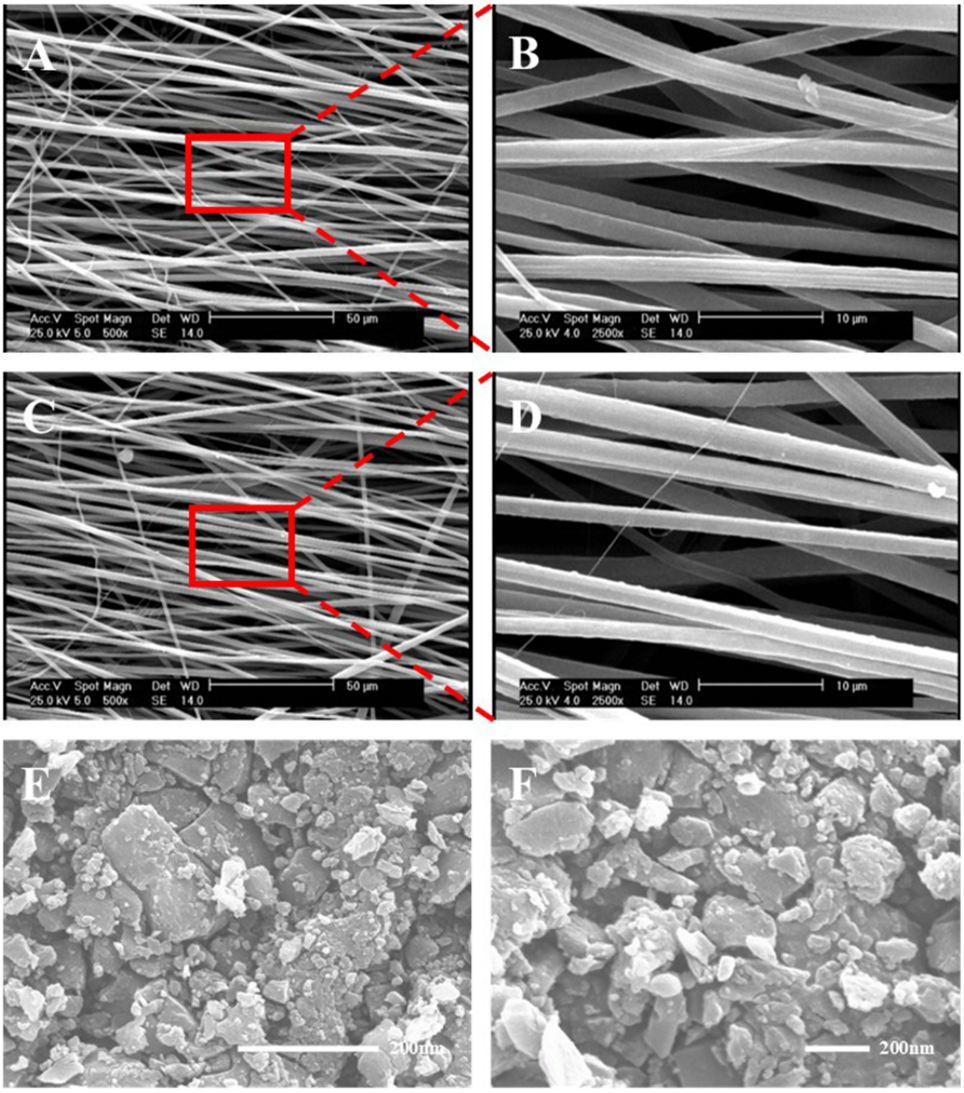

Figure 1 Representative SEM images of PCLCOLCELL scaffolds (**A-D**), ZIF-8 nanoparticles (**E**), and CURZIF-8 nanoparticles (**F**).

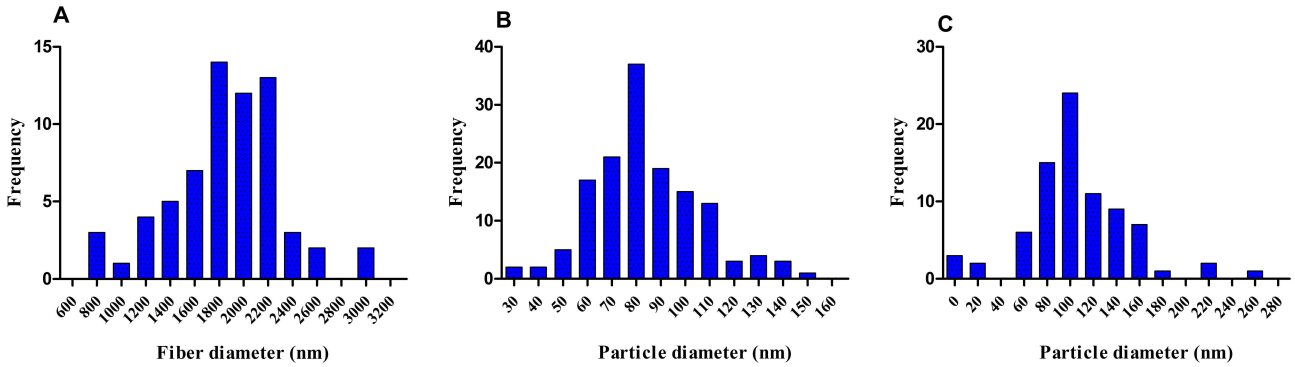

Figure 2 Size distribution of (**A**) PCLCOLCELL scaffolds, (**B**) ZIF-8 nanoparticles, and (**C**) CURZIF-8 nanoparticles.

Anti-Inflammatory Assay Results

Results (Figure 5) showed that the concentrations of proinflammatory cytokines in the COLPDLSCZIF-8-10 and control groups were significantly higher than the COLPDLSCZIF-8-1 and COLPDLSCZIF-8-2 groups. The concentrations of

https://doi.org/10.2147/IJN.S492274

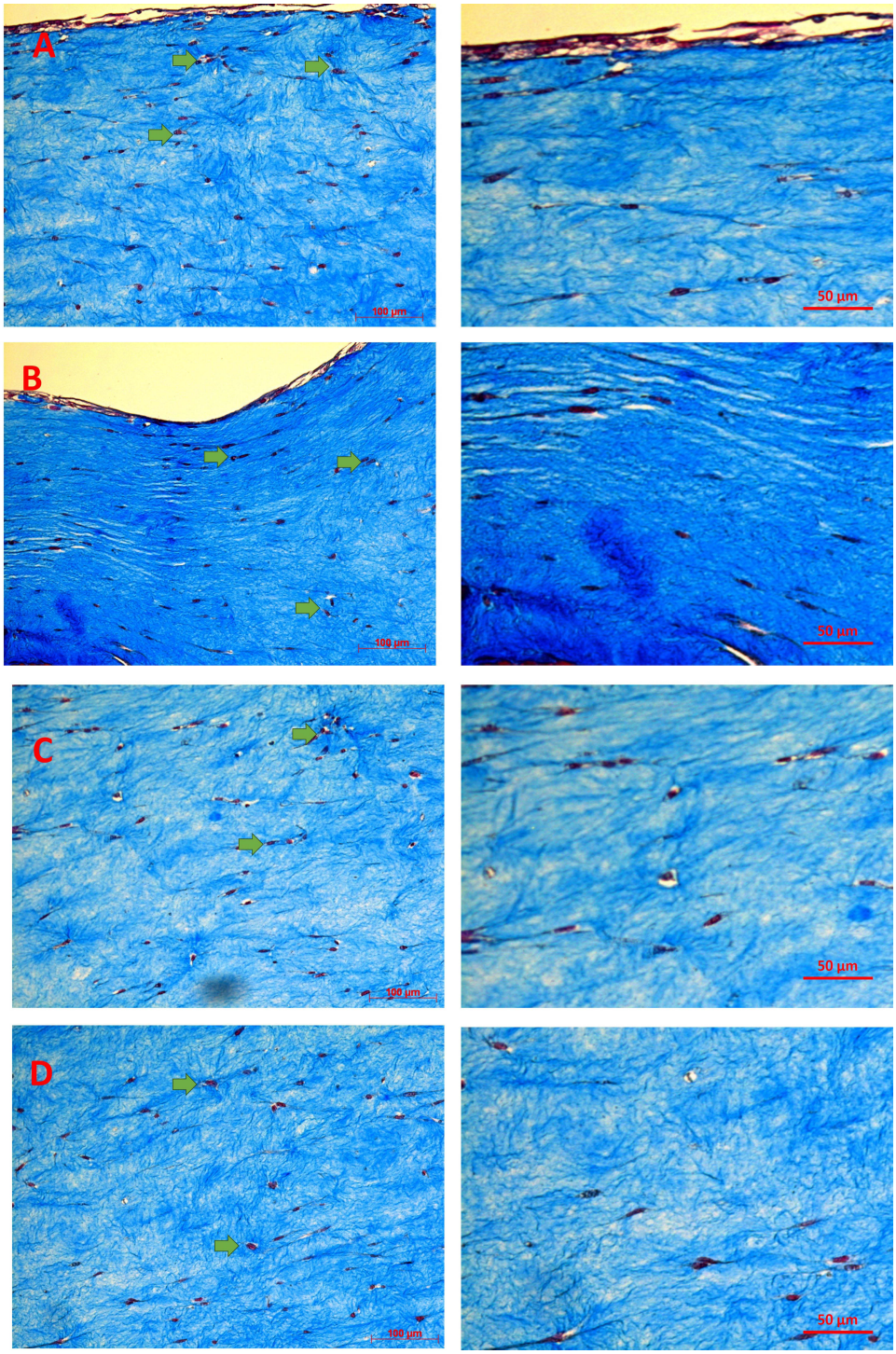

Figure 3 Representative Masson's trichrome staining images of (**A**) COLPDLSCZIF-8-1, (**B**) COLPDLSCZIF-8-2, (**C**) COLPDLSCZIF-8-10, and (**D**) PDLSCs-loaded collagen hydrogels without ZIF-8 nanoparticles. Arrows show the PDLSCs encapsulated within the hydrogel matrix.

IL-6 and IL-1β between the COLPDLSCZIF-8-1 and COLPDLSCZIF-8-2 groups were not statistically significant. TNF-α concentration in the COLPDLSCZIF-8-2 group was significantly lower than the COLPDLSCZIF-8-1 group.

Swelling Assay Results

Results (Figure 6) showed that the COLPDLSCZIF-8-1, COLPDLSCZIF-8-2, and COLPDLSCZIF-8-10hydrogels had a similar swelling pattern when incubated in complete culture media. At hour 2, the swelling percentage for

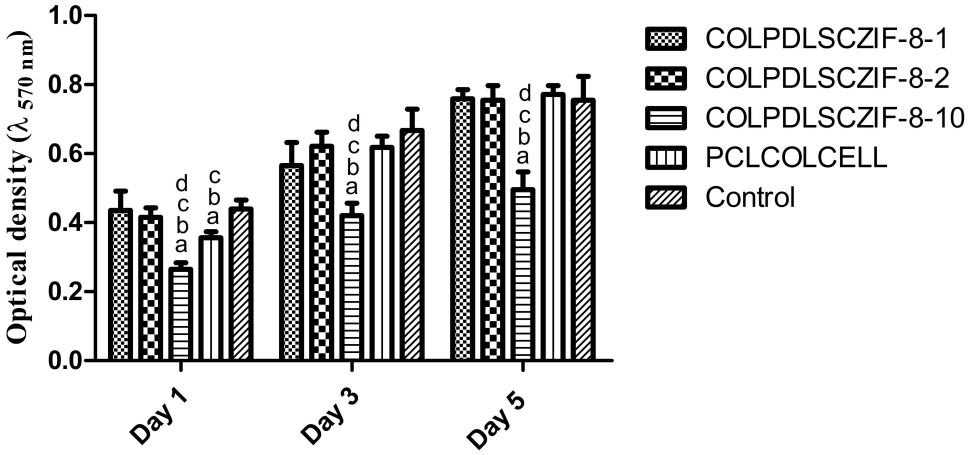

Figure 4 MTT assay results with PDLSCs cultured on/in electrospun and hydrogel scaffolds during 5-days culture period. a, b, c, and d show p-value < 0.05 relative to COLPDLSCZIF-8-1, COLPDLSCZIF-8-2, COLPDLSCZIF-8-10, and control groups, respectively.

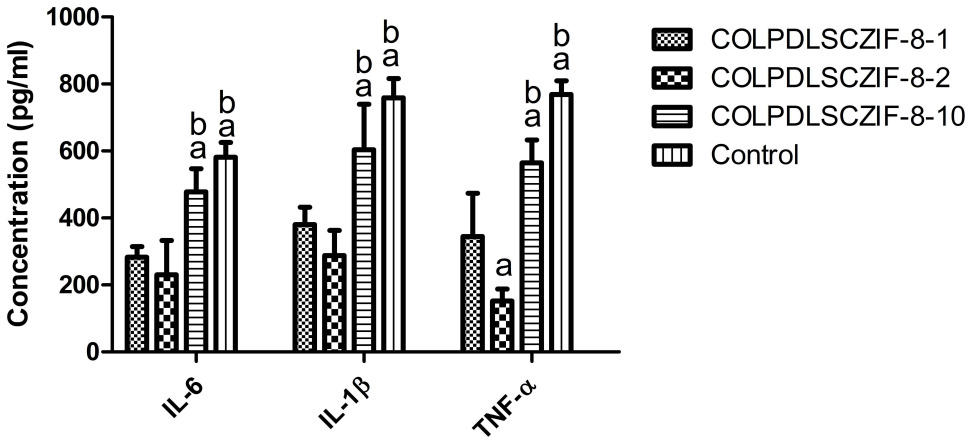

Figure 5 The anti-inflammatory activity of J774A.1 cells cultured on the COLPDLSCZIF-8-1, COLPDLSCZIF-8-2, and COLPDLSCZIF-8-10 hydrogels. The cells cultured on the tissue culture plate served as the control. a and b show p-value < 0.05 relative to COLPDLSCZIF-8-1 and COLPDLSCZIF-8-2 groups, respectively.

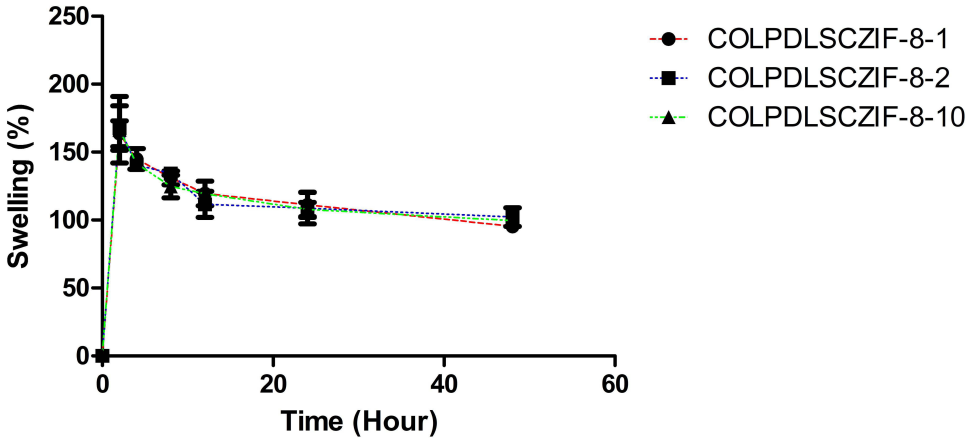

Figure 6 Swelling behavior of COLPDLSCZIF-8-1, COLPDLSCZIF-8-2, and COLPDLSCZIF-8-10 hydrogels while being incubated in complete culture media for 48 hours.

https://doi.org/10.2147/IJN.S492274

COLPDLSCZIF-8-1, COLPDLSCZIF-8-2, and COLPDLSCZIF-8-10hydrogels was measured to be around 163.54 ± 9.51, 167.71 ± 16.41, and 166.43 ± 24.52, respectively. From this time point on, the swelling percentage for all of the hydrogels started to diminish and reached its minimum level at the end of the 48th hour post-immersion in culture media.

DPPH Assay Results

Results (Figure 7) showed that at all concentrations, the radical scavenging activity of ascorbic was significantly higher than the ZIF-8 and CURZIF-8 nanoparticles. In addition, the CURZIF-8 nanoparticles had significantly higher radical scavenging activity than the ZIF-8 nanocarriers.

Cytoprotection Assay

Results (Figure 8) showed that under oxidative stress, fibroblast cells cultured with the conditioned media of COLPDLSCZIF-8-2hydrogels had significantly higher viability compared to other groups. This result implies that the COLPDLSCZIF-8-2hydrogel system had higher protective effects against oxidative stress.

Release Assay Results

Results (Figure 9) indicated that curcumin was released from CURZIF-8 nanoparticles in a sustained manner. There were two distinct phases of drug release: an initial rapid release phase and a subsequent sustained release phase. In the first few hours, a burst release occurred, resulting in 29.27 ± 3.98% of the drug being released by the 12th hour of immersion in PBS. Following this, the release rate gradually increased, reaching 77.84 ± 4.97% by the 168th hour.

Cell Migration Assay

Results (Figure 10) showed that at the 24th hour, there was no statistically significant difference in the migration activity of PDLSCs among the studied groups. However, by the 48th hour, all hydrogels exhibited significantly higher migration activity compared to the control group. Statistically, no significant difference was found among the hydrogel systems.

FTIR Assay Results

The FTIR spectra of ZIF-8 nanoparticles (Figure 11) displayed characteristic peaks corresponding to its structural components. The presence of the Zn–N bond in the imidazole ring was confirmed by a distinct peak observed around 421 cm^{-1}. Peaks at 3135 cm^{-1} and 2929 cm^{-1} were attributed to the C–H stretching vibrations of the aromatic ring and

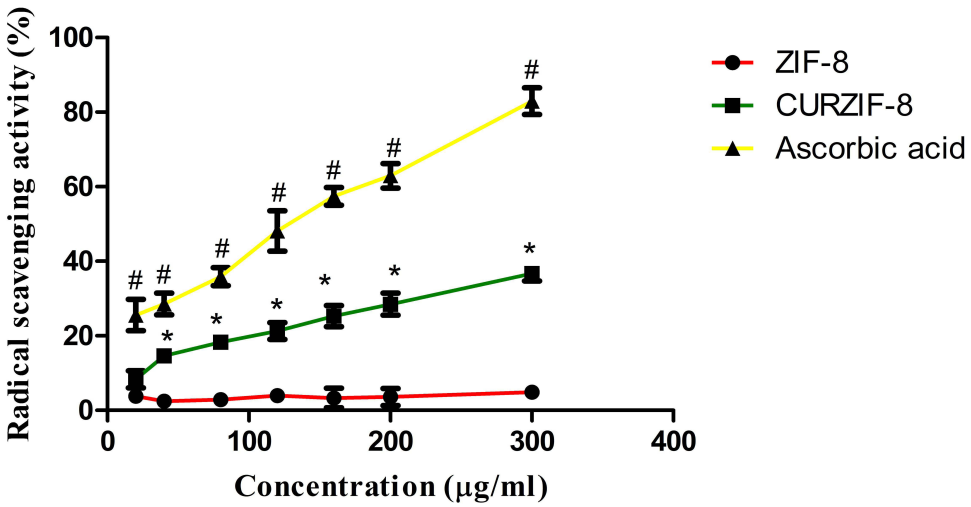

Figure 7 Radical scavenging activity of ZIF-8 and CURZIF-8 nanoparticles compared with ascorbic acid as the control. # indicates p-value < 0.05 relative to ZIF-8 and CURZIF-8 groups, and *indicates p-value < 0.05 relative to the ZIF-8 group.

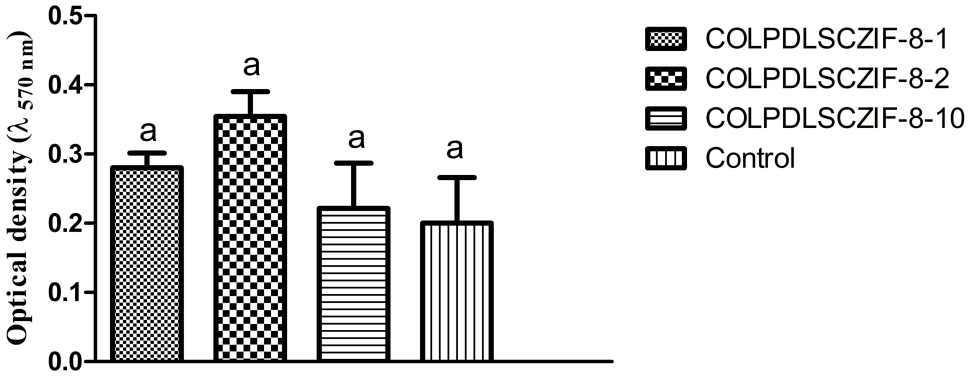

Figure 8 MTT assay with L929 fibroblast cells under oxidative stress induced by 1% v/v H_2O_2. a indicates p-value < 0.05 relative to the COLPDLSCZIF-8-2 group.

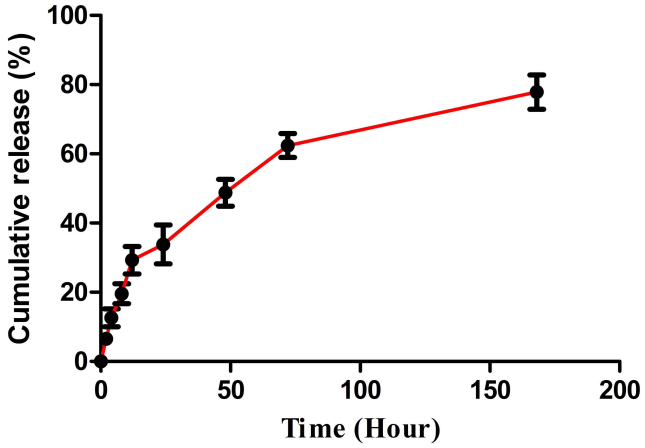

Figure 9 Release of curcumin from CURZIF-8 nanoparticles immersed in PBS for 7 days. Acquired by UV-visible spectroscopy at 420 nm.

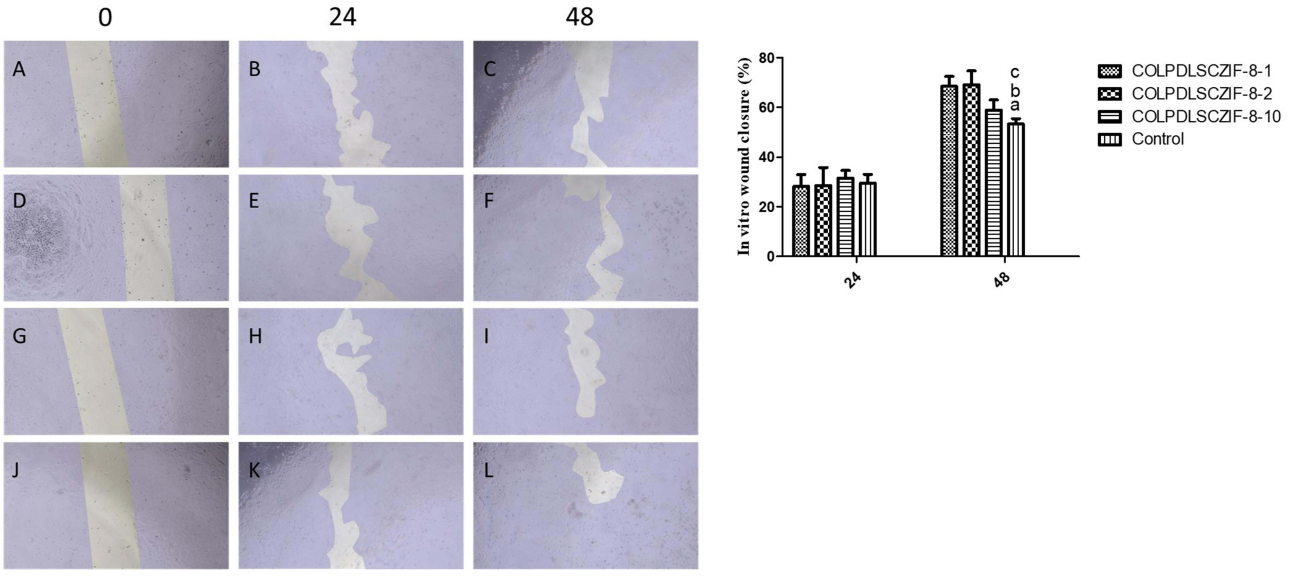

Figure 10 Migration activity of the PDLSCs in control group (**A-C**), COLPDLSCZIF-8-1 group (**D-F**), COLPDLSCZIF-8-2 group (**G-I**), COLPDLSCZIF-8-10 group (**J-L**), control is the cells cultured with the normal culture media. a, b, and c show p-value < 0.05 relative to COLPDLSCZIF-8-1, COLPDLSCZIF-8-2, and COLPDLSCZIF-8-10 groups, respectively.

https://doi.org/10.2147/IJN.S492274

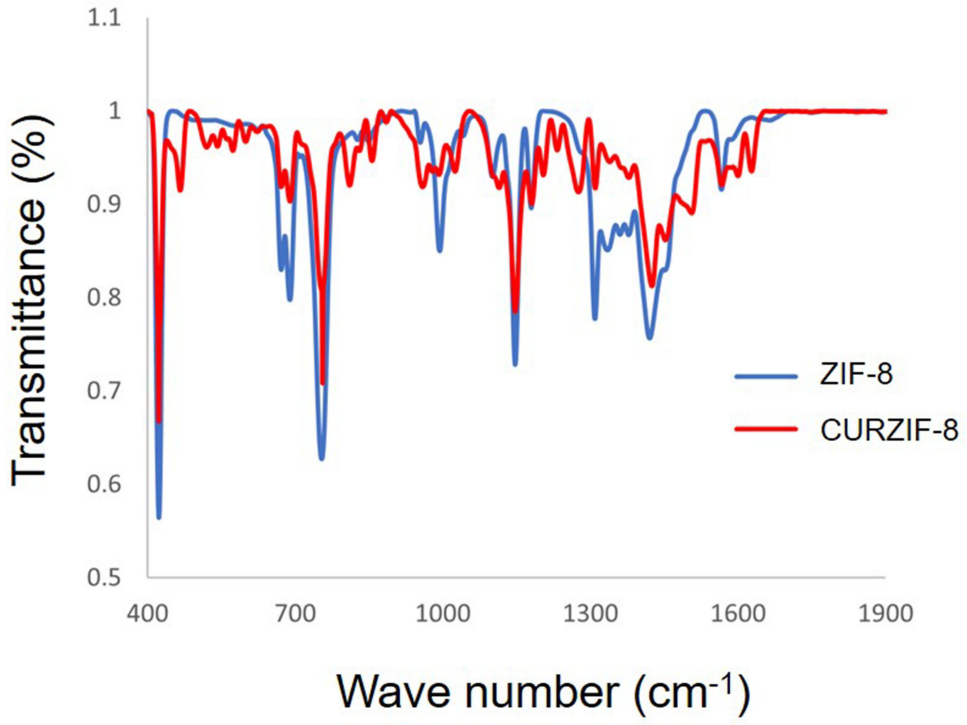

Figure 11 FTIR spectra of ZIF-8 and CURZIF-8 nanoparticles.

aliphatic chain, respectively. Additionally, the peaks around 1584 cm^{-1} and 1146 cm^{-1} were associated with the C=N stretching and C–N stretching vibrations of the imidazole ring.

In the FTIR spectra of CURZIF-8 nanoparticles, additional peaks were observed alongside those characteristics of ZIF-8, indicating successful loading of curcumin into the ZIF-8 framework. The prominent peak at around 1627 cm^{-1} was attributed to the C=O stretching vibration of the curcumin, which overlapped with the C=N stretching vibration of the ZIF-8 framework. Furthermore, peaks at 1508 cm^{-1} and 1275 cm^{-1} were indicative of the aromatic C=C stretching and C–O stretching vibrations of curcumin, respectively. The presence of these peaks confirmed the incorporation of curcumin into the ZIF-8 structure. The broadening and slight shifts in the peaks at 3135 cm^{-1} and 2929 cm^{-1} suggested interactions between the curcumin and the ZIF-8 framework, possibly through hydrogen bonding or van der Waals forces.

In vivo Study Results

Histological Evaluation Results

H&E staining images of the sham control group (Figure 12) demonstrated that cells and fibers were evenly distributed, and the PDL was well-integrated from multiple angles towards the tooth root. In the HYDELC-CELLs-CURZIF-8 group, there was a notable accumulation of osteoblasts near the newly formed bone, and the newly formed PDLs were directionally oriented, connecting the bone and the root surface. In the HYDELC-CURZIF-8 group, clusters of osteoblasts were evident, indicating bone formation; however, the new PDLs were not prominently observed. The HYDELC-CELLs group showed localized accumulation of osteoblast cells and attachment of PDLs to the root surface in some areas. In the negative control group, the distribution of cells and fibers was disorganized, with newly formed PDLs being multi-directional and lacking a clear connection to the tooth root.

Masson's trichrome staining images (Figure 13) corroborated these observations. In the sham control group, the PDL appeared uniformly integrated, with a consistent orientation towards the tooth root. The HYDELC-CELLs-CURZIF-8 group exhibited a structured arrangement of osteoblasts and newly formed PDLs, indicating successful integration with the bone and root surface. Conversely, the HYDELC-CURZIF-8 group displayed significant osteoblast activity and bone

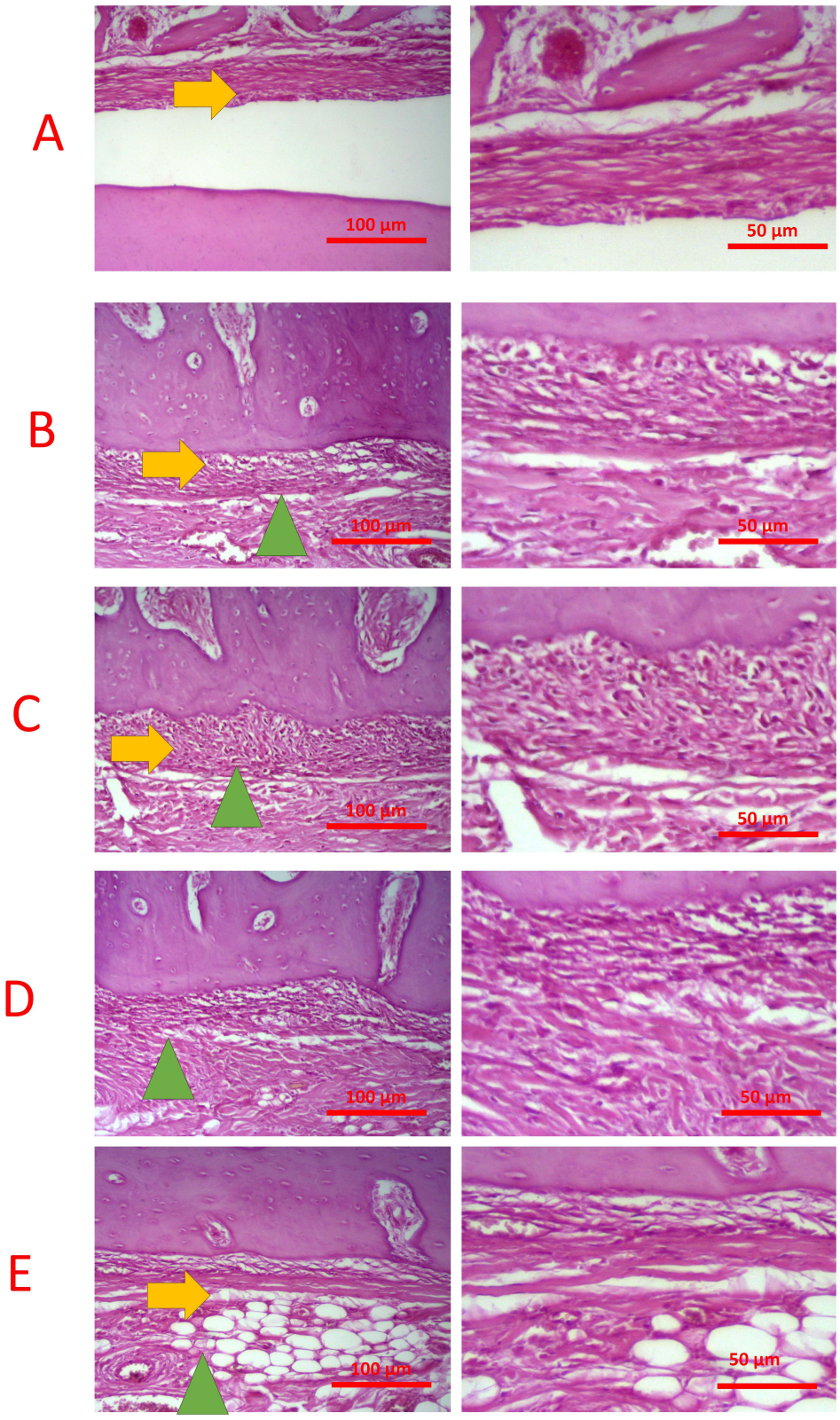

Figure 12 Representative H&E images of periodontal ligament tissue in (**A**) sham control group, (**B**) HYDELC-CELLs-CURZIF-8 group, (**C**) HYDELC-CURZIF-8 group, (**D**) HYDELC-CELLs group, and (**E**) negative control group. Arrows show periodontal ligament and arrow heads show connective tissue.

https://doi.org/10.2147/IJN.S492274

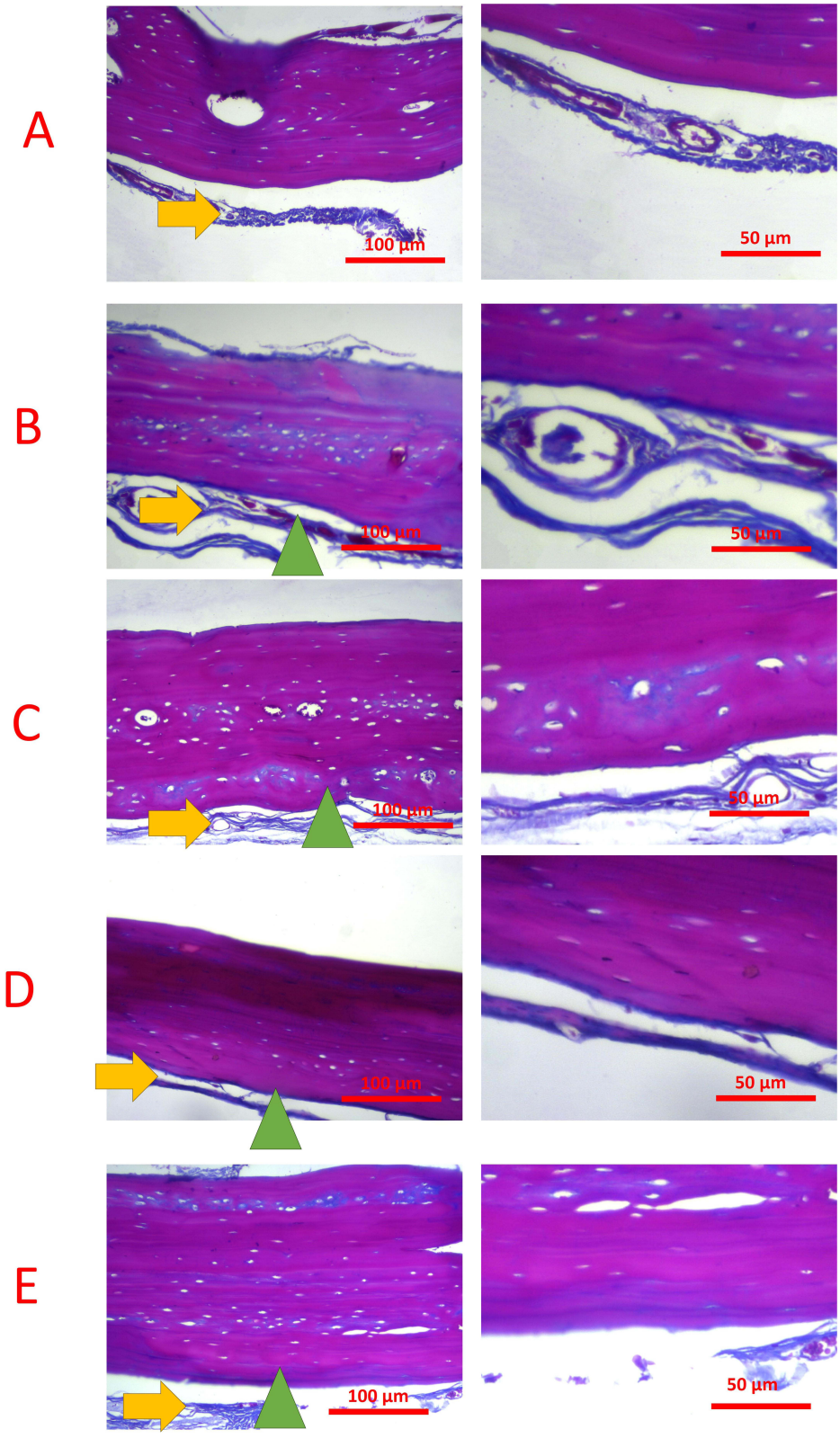

Figure 13 Representative Masson's trichrome staining images of periodontal ligament tissue in the (**A**) sham control group, (**B**) HYDELC-CELLs-CURZIF-8 group, (**C**) HYDELC-CURZIF-8 group, (**D**) HYDELC-CELLs group, and (**E**) negative control group. Arrows show periodontal ligament and arrow heads show connective tissue.

formation, but the formation of new PDLs was minimal. The HYDELC-CELLs group showed partial PDL attachment to the root surface, with osteoblast accumulation in specific areas. The negative control group presented a disordered cell and fiber distribution, with multi-directional PDLs that lacked proper integration with the tooth root.

Histomorphometry Analysis

Results (Figure 14) showed that the percentage of new bone, cementum, and periodontal ligament formation in the HYDELC-CELLs-CURZIF-8 group was significantly higher than in the other experimental groups. These values in the HYDELC-CURZIF-8 and HYDELC-CELLs groups were significantly higher than in the negative control group. The percentage of junctional epithelium and connective tissue in the HYDELC-CELLs-CURZIF-8 group was significantly lower than in the other hydrogel and negative control groups. These values in the HYDELC-CURZIF-8 and HYDELC-CELLs groups were significantly lower than in the negative control group.

ELISA Assay Results

Results (Figure 15) showed that the tissue concentrations of TGF-β, b-FGF, and HGF in the HYDELC-CELLs-CURZIF-8 group were significantly higher than in the HYDELC-CURZIF-8, HYDELC-CELLs, and negative control groups. In addition, the tissue concentrations of IL-6 and TNF-α in the HYDELC-CELLs-CURZIF-8 group were significantly lower than in the HYDELC-CURZIF-8, HYDELC-CELLs, and negative control groups. The sham control group had significantly higher tissue expression levels of TGF-β, b-FGF, and HGF than the other groups. This group also had significantly lower tissue concentrations of IL-6 and TNF-α than the other experimental groups.

Discussion

Hydrogels are considered as potential materials for the restoration and regeneration of the periodontal ligament owing to their distinctive characteristics and capacity to replicate the extracellular matrix. In this context, the cell and drug-delivering hydrogel systems are of paramount importance.[34,35] In the current research, we utilized a nanocomposite delivery system for PDLSCs and curcumin to accelerate the healing process in a rat model of periodontal ligament injury. The developed hydrogels had a fibrous architecture and provided a non-toxic environment for PDLSCs growth. SEM images showed the ECM-like architecture of electrospun scaffolds. These constructs have been shown to promote the adhesion and proliferation of PDLCs. Hua et al showed that electrospun PLA/PCL scaffolds augmented the adhesion and proliferation of PDLSCs in vitro.[36] Indeed, collagen hydrogel enables effective cell delivery and supports cell viability, proliferation, and differentiation

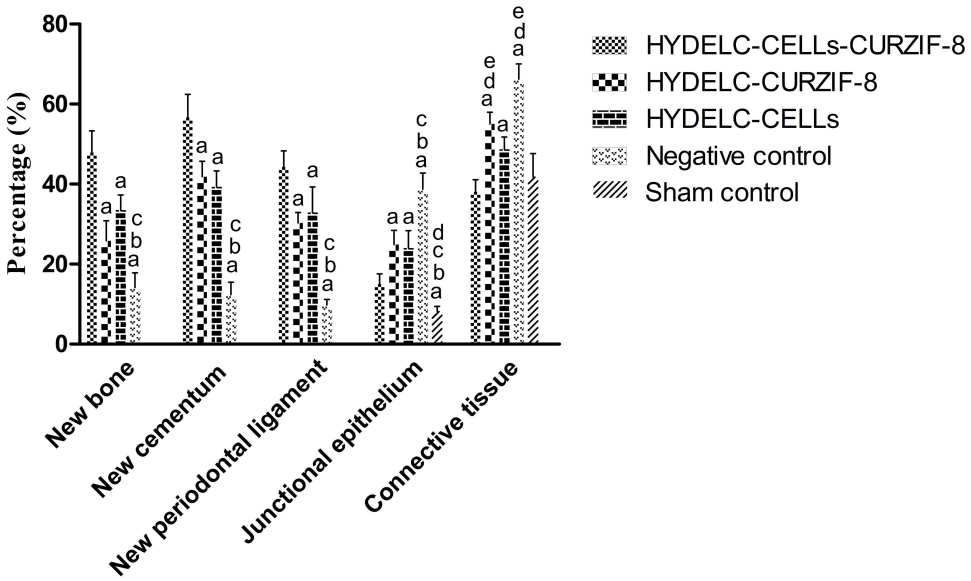

Figure 14 Histomorphometry analysis using the H&E-stained images of tissue slides in different experimental groups. a, b, c, d, and e show p-value < 0.05 relative to HYDELC-CELLs-CURZIF-8, HYDELC-CURZIF-8, HYDELC-CELLs, negative control, and sham control groups, respectively.

https://doi.org/10.2147/IJN.S492274

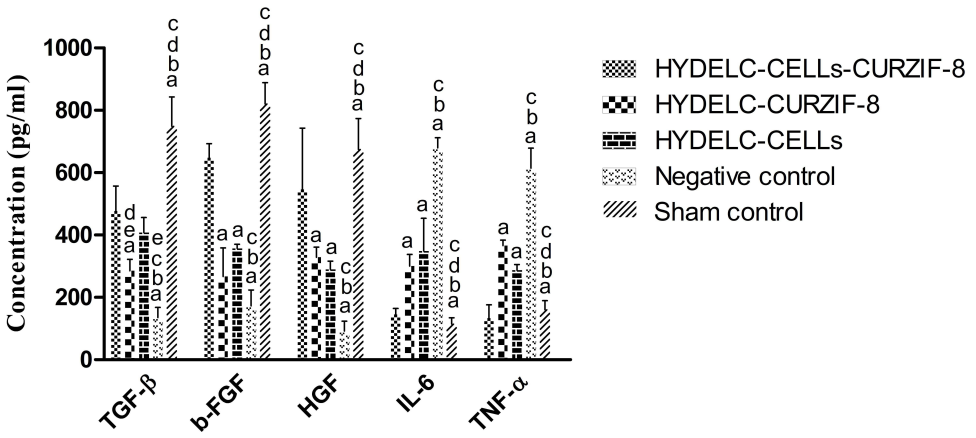

Figure 15 ELISA assay results in the periodontal ligament tissues treated with different hydrogel systems. a, b, c, d, and e show p-value < 0.05 relative to HYDELC-CELLs-CURZIF-8, HYDELC-CURZIF-8, HYDELC-CELLs, negative control, and sham control groups, respectively.

for tissue engineering and regenerative medicine applications. Ivanov et al showed that PDLSCs differentiated into osteoblast-like and odontoblast-like cells cultured in a type I collagen hydrogel.[37] Cell toxicity assay showed that the developed hydrogels were generally non-toxic against PDLSCs. However, our results indicated that COLPDLSCZIF-8-10hydrogels reduced the viability of these cells. It could be that at higher concentrations, ZIF-8 nanoparticles exhibit dose-dependent toxicity. Yang et al showed that at higher concentrations, ZIF-8 nanocarriers imparted significant tissue toxicity in corbicula fluminea.[38] The toxicity of ZIF-8 is primarily associated with the buildup of zinc inside cells. Excessive zinc accumulation results in increased reactive oxygen species (ROS) levels and cellular inflammation that eventually causes necrocytosis.[39] Although HFIP is known to be toxic to mammalian cells, our cell viability assay demonstrated that the method used to remove residual HFIP from the matrix of electrospun scaffolds was effective. As a result, these constructs did not exhibit significant toxicity toward PDLSCs. Anti-inflammatory assay results showed that the COLPDLSCZIF-8-2 had significantly higher immunomodulatory activity compared with other samples. This result can be attributed to the presence of PDLSCs and curcumin in these hydrogels. Curcumin suppresses the NF-κB pathway which is a key controller of inflammatory responses.[40] It also inhibits other inflammatory pathways like MAPK, AP-1, and JAK/STAT.[41] Curcumin reduces the production of inflammatory prostaglandins by inhibiting cyclooxygenase-2 (COX-2) and microsomal prostaglandin E synthase-1.[42] PDLSCs secrete soluble factors including TGF-β, HGF, and IDO which suppress inflammatory cells proliferation.[43] In addition, these cells can reduce T lymphocyte growth and decrease the generation of pro-inflammatory molecules such as TNF-α and IFN-γ. They encourage a transition from pro-inflammatory Th17 cells to anti-inflammatory regulatory T cells.[44,45] The swelling behavior observed in our developed hydrogels likely reflects the system reaching a swelling equilibrium. This phenamenon ensures optimal hydration and mechanical stability within the periodontal lesion. This initial swelling is beneficial as it allows the scaffold to conform closely to the defect site. Additionally, the gradual decrease in swelling over time can be attributed to the controlled degradation of the hydrogel matrix. This degradation facilitates the sustained release of therapeutic agents and provides a dynamic environment that supports tissue regeneration and healing.[19] The radical scavenging assay indicated a significant improvement in the antioxidative function of the ZIF-8 nanoparticles when loaded with curcumin. Curcumin's primary antioxidant mechanism involves donating hydrogen atoms from its phenolic OH groups and the methylene CH2 group in its β-diketone moiety to neutralize free radicals.[46,47] Additionally, curcumin can transfer single electrons to free radicals and form stabilized curcumin radicals through resonance. It can also undergo sequential hydrogen abstraction and addition reactionsand scavenge up to eight hydroxyl radicals per molecule.[48] Cytoprotection assay showed that the cells cultured with the conditioned media of COLPDLSCZIF-8-2hydrogels had significantly higher viability under oxidative stress conditions. This result could be attributed to the protective effects of curcumin and PDLSCs secretome against oxidative stress. Curcumin has been shown to mitigate oxidative stress-induced mitochondrial damage by enhancing parkin-dependent mitophagy via the AMPK-TFEB pathway.[49] While the exact mechanisms remain unclear, it has been demonstrated that stromal cell-derived factor 1 (SDF-1) can shield cells from apoptosis caused by oxidative stress.[50,51] Under

physiological conditions, the drug release from ZIF-8 nanoparticles occurs through diffusion mechanism. The sustained drug release maintains the bioactive agents bioavailability and enhance their therapeutic index.[52] Cell migration assay showed that the migration activity of PDLSCs cultured with the conditioned media of the COLPDLSCZIF-8-2hydrogels was significantly higher than other groups. Curcumin has been found to boost the growth and migration of stromal cells. This process occurs via the suppression of glycogen synthase kinase-3 beta (GSK3-β) and stabilizes β-catenin. The stabilized β-catenin then enhances cell proliferation and migration.[53] Banlue et al demonstrated that conditioned media from PDLSCs enhanced the migration activity and collagen production of human gingival fibroblast cells.[54] The curcumin-specific peaks that appeared in the FTIR spectra confirm the successful integration of curcumin within the ZIF-8 nanoparticles. It appears that the mechanism of drug loading within ZIF-8 nanoparticles is due to physical encapsulation inside the pores.[27] The in vivo study results showed that the HYDELC-CELLs-CURZIF-8 group had significantly higher healing function compared to other experimental groups. This observed healing effect may be attributed to the synergistic healing potential of curcumin and PDLSCs. PDLSCs have the ability to transform into multiple cell types essential for the restoration of periodontal tissues such as cementoblasts, osteoblasts, and fibroblasts. When integrated with appropriate scaffolding materials, they are capable of generating structures similar to the periodontal ligament and tissue resembling cementum on dentin surfaces.[55] Chang et al demonstrated that collagen scaffolds loaded with PDLSCs enhanced periodontal regeneration in a rat model.[56] Clinical studies have shown that autologous transplantation of PDLSC sheets, combined with β-tricalcium phosphate granules led to a significant improvements in periodontal pocket depth, clinical attachment level, and radiographic bone height in patients suffering from severe alveolar bone defects.[57] Curcumin has been shown to enhance the osteogenic differentiation of PDLSCs. In a study, treating these cells with 10μmol/L of curcumin significantly boosted cell viability, alkaline phosphatase activity, mineralization, and the expression of osteogenic markers such as RUNX2, osteocalcin, osteopontin, and collagen I. The osteogenic effects of curcumin on PDLSCs are thought to be mediated by the upregulation of the early growth response gene 1.[58] Recent studies have investigated the use of curcumin-primed PDLSC -derived extracellular vesicles for enhancing periodontal regeneration. These vesicles demonstrated a stronger pro-osteogenic capacity compared to standard PDLSC-derived extracellular vesicles. The enhanced osteogenic effects of these vesicles were attributed to the activation of the Wnt/β-catenin signaling pathway.[59] Therefore, it is possible that curcumin influenced the composition of PDLSC-derived vesicles and enhanced their healing activity. Our ELISA assay results implied that downregulation of inflammation and upregulation of pro-healing factors contributed to the observed healing effects. TGF-β, b-FGF, and HGF are crucial growth factors involved in tissue repair. TGF-β regulates cell proliferation and differentiation that aid in wound healing.[60] b-FGF promotes angiogenesis and tissue regeneration.[61] HGF enhances cell migration and growth and contribute to tissue repair and regeneration.[62] Together, these factors play a vital role in healing and restoring damaged tissues. It is also possible that other signaling pathways contributed to the observed healing effects that were not examined in this study and require further investigation. Understanding these pathways could provide a more comprehensive insight into the mechanisms behind the enhanced regenerative capabilities PDLSCs when delivered locally with curcumin-loaded nanocomposite scaffolds. In a similar approach to our study, Wang et al developed an aligned porous hydrogel scaffold and loaded it with PDLSCs or gingival mesenchymal stem cells (GMSCs) to treat periodontitis. The scaffold demonstrated biocompatibility with both cell types in vitro and showed enhanced bone tissue repair and periodontal ligament formation in a rat periodontal defect model. Immunohistochemical analysis revealed upregulation of osteogenic markers in treated groups.[55] A kato et al evaluated the effects of combining bone morphogenetic protein (BMP-2) modification with collagen hydrogel scaffold implantation on periodontal wound healing in dogs.[63] One-wall infrabony defects were surgically created in six beagle dogs and treated with either BMP-2, collagen hydrogel scaffolds, or a combination of both. BMP-2 alone promoted alveolar bone formation but caused ankylosis. In contrast, the combination treatment significantly enhanced periodontal attachment regeneration. Our proposed approach for periodontal regeneration offers notable advancements over traditional methods. This system effectively supports PDLSCs delivery, enhances anti-inflammatory and antioxidative activities, and promotes organized tissue regeneration. Unlike GTR and barrier membranes, which often fail to restore the full functionality of periodontal tissues, the proposed method achieves improved bone-cementum integration and a more robust regenerative outcome. The sustained drug release of curcumin encapsulated in ZIF-8 nanoparticles addresses rapid degradation issues seen in earlier delivery systems while enhancing PDLSC-mediated tissue repair. However, the preclinical nature of this study limits the direct applicability of findings to humans. The dose-dependent toxicity of ZIF-8 nanoparticles also necessitates further optimization to ensure safety without compromising

efficacy. While short-term results are promising, the lack of long-term data on the stability and functionality of regenerated tissues highlights the need for extended studies. Future work should focus on refining scaffold composition, testing in larger animal models, and initiating clinical trials to validate this method's potential for therapeutic application.

Conclusion

Our findings indicate that the developed system provided a protective environment for PDLSCs against oxidative stress. In vivo experiments conducted in a rat model underscored the system's efficacy in promoting robust PDL regeneration. This was evidenced by histological assessments tgat revealed enhanced tissue architecture and ELISA analyses demonsted the increased expression of essential growth factors such as bFGF, HGF, and TGF-β. Concurrently, the observed decrease in pro-inflammatory cytokines TNF-α and IL-6 further validated the anti-inflammatory properties of the delivery system. The outcomes of this study suggest that our developed approach holds promise as an advanced strategy for augmenting PDL repair mechanisms through targeted modulation of inflammation and promotion of pro-healing factors within the periodontal microenvironment. Future research efforts should focus on further optimizing the scaffold design and exploring long-term efficacy and safety in larger animal models.

Data Sharing Statement

All data generated or analysed during this study are included in this published article.

Code Availability

In this work, only public software and custom code were used to generate or process datasets. The software version and websites were described in the "Methods" section.

Ethics Declarations

This study was approved by the Ethical Committee of Shanxi Bethune Hospital (Approval No. YXLL-2023-322). All procedures involving animals were reviewed and approved by the Institutional Animal Care and Use Committee by the of the Ethics Committee of Shanxi Province Hospital of Traditional Chinese medicine. China's Guidelines for the Ethical Review of Laboratory Animal Welfare were followed for the welfare of the laboratory animals. ARRIVE guidelines have been followed for the in vivo study.

Acknowledgments

This study received no funding.

Disclosure

All authors declare no financial or non-financial competing interests.

References

1. Usui M, Onizuka S, Sato T, et al. Mechanism of alveolar bone destruction in periodontitis—periodontal bacteria and inflammation. *Japan Dent Sci Rev*. 2021;57:201–208. doi:10.1016/j.jdsr.2021.09.005
2. Łasica A, Golec P, Laskus A, et al. Periodontitis: etiology, conventional treatments, and emerging bacteriophage and predatory bacteria therapies. *Front Microbiol*. 2024;15:1469414. doi:10.3389/fmicb.2024.1469414
3. Ward E. A review of tissue engineering for periodontal tissue regeneration. *J Vet Dent*. 2022;39(1):49–62. doi:10.1177/08987564211065137
4. Yao Y, Raymond JE, Kauffmann F, et al. Multicompartmental scaffolds for coordinated periodontal tissue engineering. *J Dent Res*. 2022;101(12):1457–1466. doi:10.1177/00220345221099823
5. Staples RJ, Ivanovski S, Vaquette C. Fibre guiding scaffolds for periodontal tissue engineering. *J Periodontal Res*. 2020;55(3):331–341. doi:10.1111/jre.12729
6. Daghrery A, Bottino MC. Advanced biomaterials for periodontal tissue regeneration. *genesis*. 2022;60(8–9):e23501. doi:10.1002/dvg.23501
7. Liu Y, Guo L, Li X, et al. Challenges and tissue engineering strategies of periodontal-guided tissue regeneration. *Tissue Eng Part C*. 2022;28(8):405–419.
8. Almeida ND, Carneiro CA, de Marco AC, et al. 3D bioprinting techniques and bioinks for periodontal tissues regeneration—A literature review. *Biomimetics*. 2024;9(8):480. doi:10.3390/biomimetics9080480
9. Magalhães FD, Sarra G, Carvalho GL, et al. Dental tissue-derived stem cell sheet biotechnology for periodontal tissue regeneration: a systematic review. *Arch Oral Biol*. 2021;129:105182. doi:10.1016/j.archoralbio.2021.105182

10. Zhang Y, Zhao W, Jia L, et al. The application of stem cells in tissue engineering for the regeneration of periodontal defects in randomized controlled trial: a systematic review and meta-analysis. *J Evid Based Dent Pract*. 2022;22(2):101713. doi:10.1016/j.jebdp.2022.101713
11. Aghandeh P, Kouhestani F, Isamorad F, et al. Efficacy of application of periodontal ligament stem cells in bone regeneration: a systematic review of animal studies. *Dent Hypotheses*. 2022;13(4):111–116. doi:10.4103/denthyp.denthyp_136_22
12. Zhang Z, Deng M, Hao M, et al. Periodontal ligament stem cells in the periodontitis niche: inseparable interactions and mechanisms. *J Leukoc Biol*. 2021;110(3):565–576. doi:10.1002/JLB.4MR0421-750R
13. Zhao X, Li Q, Guo Z, et al. Constructing a cell microenvironment with biomaterial scaffolds for stem cell therapy. *Stem Cell Res Ther*. 2021;12 (1):1–13. doi:10.1186/s13287-021-02650-w
14. Stojanov S, Berlec A. Electrospun nanofibers as carriers of microorganisms, stem cells, proteins, and nucleic acids in therapeutic and other applications. *Front Bioeng Biotechnol*. 2020;8:130. doi:10.3389/fbioe.2020.00130
15. Liu Z, Ramakrishna S, Liu X. Electrospinning and emerging healthcare and medicine possibilities. *APL Bioeng*. 2020;4(3). doi:10.1063/5.0012309
16. Rahmati M, et al. Electrospinning for tissue engineering applications. *Pro Mater Sci*. 2021;117:100721.
17. Perez-Puyana V, Wieringa P, Yuste Y, et al. Fabrication of hybrid scaffolds obtained from combinations of PCL with gelatin or collagen via electrospinning for skeletal muscle tissue engineering. *J Biomed Mater Res Part A*. 2021;109(9):1600–1612. doi:10.1002/jbm.a.37156
18. Salehi AOM, Heidari Keshel S, Sefat F, et al. Use of polycaprolactone in corneal tissue engineering: a review. *Mater Today Commun*. 2021;27:102402. doi:10.1016/j.mtcomm.2021.102402
19. Lanza R, Langer R, Vacanti JP, Atala A. *Principles of Tissue Engineering*. Academic press; 2020.
20. Wang Y, Wang Z, Dong Y. Collagen-based biomaterials for tissue engineering. *ACS Biomater Sci Eng*. 2023;9(3):1132–1150. doi:10.1021/acsbiomaterials.2c00730
21. Laboy-López S, Méndez Fernández PO, Padilla-Zayas JG, et al. Bioactive cellulose acetate electrospun mats as scaffolds for bone tissue regeneration. *Int J Biomater*. 2022;2022(1):3255039. doi:10.1155/2022/3255039
22. Ren J, Fok MR, Zhang Y, et al. The role of non-steroidal anti-inflammatory drugs as adjuncts to periodontal treatment and in periodontal regeneration. *J Transl Med*. 2023;21(1):149. doi:10.1186/s12967-023-03990-2
23. Zheng D, Huang C, Huang H, et al. Antibacterial mechanism of curcumin: a review. *Chem Biodivers*. 2020;17(8):e2000171. doi:10.1002/cbdv.202000171
24. Quispe C, Herrera-Bravo J, Javed Z, et al. Therapeutic applications of curcumin in diabetes: a review and perspective. *Biomed Res Int*. 2022;2022 (1):1375892. doi:10.1155/2022/1375892
25. Pan-On S, Dilokthornsakul P, Tiyaboonchai W. Trends in advanced oral drug delivery system for curcumin: a systematic review. *J Control Release*. 2022;348:335–345. doi:10.1016/j.jconrel.2022.05.048
26. Zheng C, Wang Y, Phua SZF, et al. ZnO–DOX@ ZIF-8 core–shell nanoparticles for pH-responsive drug delivery. *ACS Biomater Sci Eng*. 2017;3 (10):2223–2229. doi:10.1021/acsbiomaterials.7b00435
27. Wang Q, Sun Y, Li S, et al. Synthesis and modification of ZIF-8 and its application in drug delivery and tumor therapy. *RSC Adv*. 2020;10 (62):37600–37620. doi:10.1039/D0RA07950B
28. Tiwari A, Singh A, Garg N, et al. Curcumin encapsulated zeolitic imidazolate frameworks as stimuli responsive drug delivery system and their interaction with biomimetic environment. *Sci Rep*. 2017;7(1):12598. doi:10.1038/s41598-017-12786-6
29. Sahiner M, Alpaslan D, Bitlisli BO. Collagen-based hydrogel films as drug-delivery devices with antimicrobial properties. *Polym Bull*. 2014;71 (11):3017–3033. doi:10.1007/s00289-014-1235-x
30. Pupkaite J, Rosenquist J, Hilborn J, et al. Injectable shape-holding collagen hydrogel for cell encapsulation and delivery cross-linked using thiol-michael addition click reaction. *Biomacromolecules*. 2019;20(9):3475–3484. doi:10.1021/acs.biomac.9b00769
31. Zheng D, Wu Z, Guan X, et al. Intervertebral disc regeneration in a rat model via nanocomposite hydrogel loaded with palette rich plasma growth factors, endometrial stem cells, and melatonin: an in vitro and in vivo study. *J Drug Delivery Sci Technol*. 2023;90:105122. doi:10.1016/j.jddst.2023.105122
32. Ye L, Gao Z, Rohani S. Intervertebral disk regeneration in a rat model by allopurinol-loaded chitosan/alginate hydrogel. *Biomole Biomed*. 2023;23 (4):661. doi:10.17305/bb.2022.8550
33. Kosen Y, Miyaji H, Kato A, et al. Application of collagen hydrogel/sponge scaffold facilitates periodontal wound healing in class II furcation defects in beagle dogs. *J Periodontal Res*. 2012;47(5):626–634. doi:10.1111/j.1600-0765.2012.01475.x
34. Chen F-M, Jin Y. *Periodontal tissue engineering and regeneration: current approaches and expanding opportunities*. *Tissue Eng Part B*. 2010;16 (2):219–255.
35. Galli M, Yao Y, Giannobile WV, et al. Current and future trends in periodontal tissue engineering and bone regeneration. *Plast Aesthetic Res*. 2021;8:3. doi:10.20517/2347-9264.2020.176
36. Hua W, Xiang J, Wu Y, et al. Growth factor-encapsulated triphasic scaffolds of electrospun polylactic acid–polycaprolactone (PLA–PCL) nanofibrous mats combined with a directionally freeze-dried chitosan hydrogel for periodontal tissue regeneration. *Mater Adv*. 2023;4 (20):4798–4811. doi:10.1039/D3MA00465A
37. Ivanov AA, Kuznetsova AV, Popova OP, et al. Influence of extracellular matrix components on the differentiation of periodontal ligament stem cells in collagen i hydrogel. *Cells*. 2023;12(19):2335. doi:10.3390/cells12192335
38. Yang C, Wen J, Xue Z, et al. The accumulation and toxicity of ZIF-8 nanoparticles in corbicula fluminea. *J Environ Sci*. 2023;127:91–101. doi:10.1016/j.jes.2022.03.020
39. Chen P, He M, Chen B, et al. Size-and dose-dependent cytotoxicity of ZIF-8 based on single cell analysis. *Ecotoxicol Environ Saf*. 2020;205:111110. doi:10.1016/j.ecoenv.2020.111110
40. Vadhan-Raj S, Weber DM, Wang M, et al. Curcumin downregulates NF-kB and related genes in patients with multiple myeloma: results of a phase I/II study. *Blood*. 2007;110(11):1177. doi:10.1182/blood.V110.11.1177.1177
41. Peng Y, Ao M, Dong B, et al. Anti-inflammatory effects of curcumin in the inflammatory diseases: status, limitations and countermeasures. *Drug Des Devel Ther*. 2021;Volume 15:4503–4525. doi:10.2147/DDDT.S327378
42. Shimizu K, Funamoto M, Sunagawa Y, et al. Anti-inflammatory action of curcumin and its use in the treatment of lifestyle-related diseases. *Eur Cardiol Rev*. 2019;14(2):117. doi:10.15420/ecr.2019.17.2

43. Wada N, Tomokiyo A, Gronthos S, et al. Immunomodulatory properties of PDLSC and relevance to periodontal regeneration. *Curr Oral Health Rep*. 2015;2(4):245–251. doi:10.1007/s40496-015-0062-y
44. Behm C, Zhao Z, Andrukhov O. Immunomodulatory activities of periodontal ligament stem cells in orthodontic forces-induced inflammatory processes: current views and future perspectives. *Front Oral Health*. 2022;3:877348. doi:10.3389/froh.2022.877348
45. Li P, Ou Q, Shi S, et al. Immunomodulatory properties of mesenchymal stem cells/dental stem cells and their therapeutic applications. *Cell Mol Immunol*. 2023;20(6):558–569. doi:10.1038/s41423-023-00998-y
46. Barzegar A, Moosavi-Movahedi AA, Calixto JB. Intracellular ROS protection efficiency and free radical-scavenging activity of curcumin. *PLoS One*. 2011;6(10):e26012. doi:10.1371/journal.pone.0026012
47. Li Y, Toscano M, Mazzone G, et al. Antioxidant properties and free radical scavenging mechanisms of cyclocurcumin. *New J Chem*. 2018;42 (15):12698–12705. doi:10.1039/C8NJ01819G
48. Agnihotri N, Mishra P. Scavenging mechanism of curcumin toward the hydroxyl radical: a theoretical study of reactions producing ferulic acid and vanillin. *J Phys Chem A*. 2011;115(49):14221–14232. doi:10.1021/jp209318f
49. Hu P, Li K, Peng -X-X, et al. Curcumin derived from medicinal homologous foods: its main signals in immunoregulation of oxidative stress, inflammation, and apoptosis. *Front Immunol*. 2023;14:1233652. doi:10.3389/fimmu.2023.1233652
50. Feng Y, Fu X, Lou X, et al. Stromal cell-derived factor 1 protects human periodontal ligament stem cells against hydrogen peroxide-induced apoptosis. *Mol Med Rep*. 2017;16(4):5001–5006. doi:10.3892/mmr.2017.7192
51. Du L, Yang P, Ge S. Stromal cell–derived factor-1 significantly induces proliferation, migration, and collagen type I expression in a human periodontal ligament stem cell subpopulation. *J Periodontol*. 2012;83(3):379–388. doi:10.1902/jop.2011.110201
52. Cai W, Zhang W, Chen Z. Magnetic Fe3O4@ ZIF-8 nanoparticles as a drug release vehicle: pH-sensitive release of norfloxacin and its antibacterial activity. *Colloids Surf B*. 2023;223:113170. doi:10.1016/j.colsurfb.2023.113170
53. Konain K, Saddique N, Samie M, et al. Curcumin-loaded nanofibrous matrix accelerates fibroblast cell proliferation and enhances wound healing via GSK3-β inhibition. *J Compos Sci*. 2023;7(8):343. doi:10.3390/jcs7080343
54. Banlue A, Kaewmuangmoon J, Janebodin K, et al. Induction of migration and collagen synthesis in human gingival fibroblasts using periodontal ligament stem cell conditioned medium. *Eur J Dent*. 2024;18(01):219–227. doi:10.1055/s-0043-1764422
55. Wang W, Wang A, Hu G, et al. Potential of an aligned porous hydrogel scaffold combined with periodontal ligament stem cells or gingival mesenchymal stem cells to promote tissue regeneration in rat periodontal defects. *ACS Biomater Sci Eng*. 2023;9(4):1961–1975. doi:10.1021/acsbiomaterials.2c01440
56. Chang Y-T, Lai -C-C, Lin D-J. Collagen scaffolds laden with human periodontal ligament fibroblasts promote periodontal regeneration in SD Rat model. *Polymers*. 2023;15(12):2649. doi:10.3390/polym15122649
57. Song IS, Han YS, Lee J-H, et al. Periodontal ligament stem cells for periodontal regeneration. *Curr Oral Health Rep*. 2015;2(4):236–244. doi:10.1007/s40496-015-0060-0
58. Tan L, Cao Z, Chen H, et al. Curcumin reduces apoptosis and promotes osteogenesis of human periodontal ligament stem cells under oxidative stress in vitro and in vivo. *Life Sci*. 2021;270:119125. doi:10.1016/j.lfs.2021.119125
59. Lan Q, Cao J, Bi X, et al. Curcumin-primed periodontal ligament stem cells-derived extracellular vesicles improve osteogenic ability through the Wnt/β-catenin pathway. *Front Cell Develop Biol*. 2023;11:1225449. doi:10.3389/fcell.2023.1225449
60. Massagué J, Sheppard D. TGF-β signaling in health and disease. *Cell*. 2023;186(19):4007–4037. doi:10.1016/j.cell.2023.07.036
61. Wu X, Guo H, Jia Y, et al. Adipose mesenchymal stem cell-based tissue engineering mesh with sustained bFGF release to enhance tissue repair. *Biomater Sci*. 2022;10(12):3110–3121. doi:10.1039/D1BM01893K
62. Xu X, Xing Q, Liu R, et al. Therapeutic effects and repair mechanism of hgf gene-transfected mesenchymal stem cells on injured endometrium. *Stem Cells Int*. 2022;2022(1):5744538. doi:10.1155/2022/5744538
63. Kato A, Miyaji H, Ishizuka R, et al. Combination of root surface modification with BMP-2 and collagen hydrogel scaffold implantation for periodontal healing in beagle dogs. *Open Dent J*. 2015;9:52. doi:10.2174/1874210601509010052